The Role of OH and HO_2 Radicals in Tropospheric Night-time Oxidation Processes: Field Observations and Modelling

Hannah Bunyan (cmhmb@leeds.ac.uk), Daniel Stone, Trevor Ingham, Stewart Vaughan, Mathew Evans and Dwayne Heard

NATURAL ENVIRONMENT RESEARCH COUNCIL

National Centre for Atmospheric Science

UNIVERSITY OF LEEDS

1 Introduction

Tropospheric Oxidation Chemistry

- The hydroxyl radical (OH) is the major oxidising chemical in the daytime troposphere, destroying ~ 3.7 Gt of trace gases, including CH_4, HFCs and HCFCs, each year (Foster *et al.*, IPCC 2007)
- Primary day-time production of OH in the troposphere occurs *via* photolysis of ozone at $\lambda < 340$ nm; Production and loss of HO_2 and OH are closely linked through radical recycling reactions
- Ozonolysis of alkenes is a known source of OH and HO_2 at night (Kanaya *et* al., 1999; Salibsury *et al.*, 2001; Geyer *et al.*, 2003; Ren *et al.*, 2003; Ren *et al.*, 2006; Sommariva *et al.*, 2007)
- Reactions of the nitrate radical (NO_3) with VOCs contribute to night-time oxidation and radical production (Salisbury *et al.*, 2001; Geyer *et al.*, 2003; Emmerson and Carslaw, 2009)

The RONOCO Project

- **RONOCO**: **R**ole **o**f **n**ight-time chemistry in controlling the **o**xidising **c**apacity of the atm**o**sphere
- Measurements of OH, HO_2, NO_3, N_2O_5 and longer-lived species were made onboard the NERC BAe-146 research aircraft, during 18 night-time flights over the UK in July 2010 and January 2011
- Aims: 1) Enhance understanding of night-time chemistry by taking comprehensive measurements of night-time composition
  2) Investigate processes controlling atmospheric night-time oxidation
  3) Investigate regional and global impact of night-time chemistry on air quality and climate change

2 The Leeds FAGE Aircraft Instrument

- **FAGE**: Fluorescence Assay by Gas Expansion (Commane *et al.*, 2010)
- Laser-induced fluorescence spectroscopy at low pressure
- Specialised inlet mounted in aircraft window blank; ambient air sampled from outside the aircraft through 0.7 mm pinhole (Figures 1 and 2)
- Laser light at $\lambda = 308$ nm excites OH radicals; fluorescence occurs at $\lambda = 308$ nm
- Fluorescence lifetime is extended as a result of reduced collisional quenching at low pressure; fluorescence is collected by time–gated photon counting
- HO_2 is detected *via* chemical conversion to OH using an excess of NO

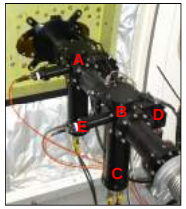

Figure 1: FAGE detection assembly installed on BAe-146 aircraft, showing OH and HO_2 fluorescence cells (A, B), photomultiplier tube (C), photodiode (D), and optical fibres delivering laser light (E).

Figure 2: BAe-146 Research Aircraft, with HO_x inlet circled in red.

3 DSMACC Box Model

- Observations of OH, HO_2, NO_3 and N_2O_5 are interpreted using the Dynamically Simple Model of Atmospheric Chemical Complexity (DSMACC) (Emmerson and Evans, 2009; Stone *et al.*, 2010)
- Zero-dimensional model constrained to observations of long-lived species
- Chemistry scheme described by the Master Chemical Mechanism (MCM v3.2) (Jenkin *et al.*, 2003; Saunders *et* al., 2003); subset used contains ~ 2000 species in ~ 8000 reactions
- Aerosol uptake of OH, HO_2, CH_3O_2, NO_3, N_2O_5 and HNO_3 included in the model
- Model run forwards until a diurnal steady state is reached
- Model calculations include representation of potential RO_2 interference in LIF measurements of HO_2 (Fuchs *et al.*, 2011); $HO_2^* = HO_2 + fRO_2$
  For RONOCO, $HO_2^* = [1.15 \times HO_2] + 2 \times 10^5$ cm^{-3}

4 Measurements

Overview of FAGE HO_x measurements

- OH was measured during 13 flights; HO_2 was measured during 16 flights
- Maximum night-time HO_2 =13.7 pptv, measured during flight on 20th July 2010
- HO_2 correlates strongly with NO_3 (Figure 3)
- OH not detected at night above the instrument's limit of detection during the summer and winter campaigns, as predicted by model (see model results in section 5)

		Average Mixing Ratio / pptv	Average Concentration / molecule cm^{-3}	Limit of Detection / molecule cm^{-3}
Summer	OH	0.04	8.9×10^5	1.8×10^6
	HO_2	1.6	3.7×10^7	6.9×10^5
Winter	OH	0.005	1.2×10^5	6.4×10^5
	HO_2	0.7	1.7×10^7	6.0×10^5

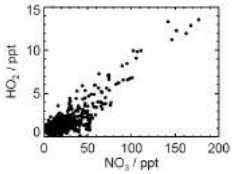

Figure 3: Correlation between measured HO_2 and NO_3 during summer flights; $R = 0.84$

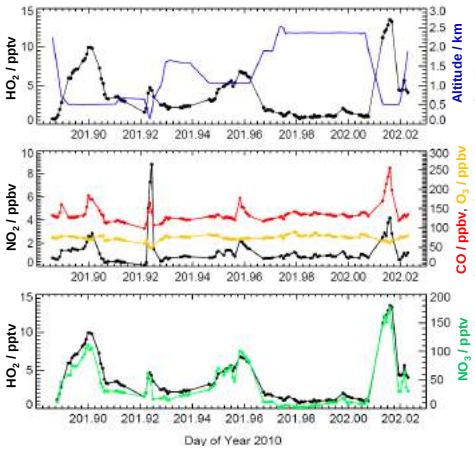

Figure 4: Time series of HO_2 and concurrent measurements during night-time flight on 20th July 2010. NO_3 data courtesy of B. Ouyang and O. Kennedy, University of Cambridge. CO, O_3, NO_2 and altitude data courtesy of FAAM.

Example of night-time flight

- Maximum night-time HO_2 ~ 13 pptv, measured during flight on 20th July 2010 (Figure 4)
- Low-level flying off the Norfolk coast and the Thames Estuary
- High levels of O_3, CO and HO_2 were measured
- HO_2 correlates strongly with NO_3 during the flight (R = 0.97) , suggesting a common source or chemical coupling

Analysis of night-time HO_2 production

- Correlation between measured HO_2 and NO_3 during some flights suggests NO_3 is important in HO_2 production at night, as shown in previous studies (e.g. Salisbury *et al.*, 2001; Geyer *et al.*, 2003; Emmerson and Carslaw, 2009)
- HO_2 and NO_3 were measured simultaneously on an aircraft for the first time in the RONOCO campaign
- Rates of production of HO_2 (P_{HO2}) calculated using the measurements
- *Trans*-2-butene, propene and isoprene are the key alkenes in HO_2 production calculated from the measurements
- Total P_{HO2} was higher during summer flights than in winter flights
- NO_3-initiated oxidation dominated HO_2 production in summer
- O_3-initiated oxidation dominated HO_2 production in winter

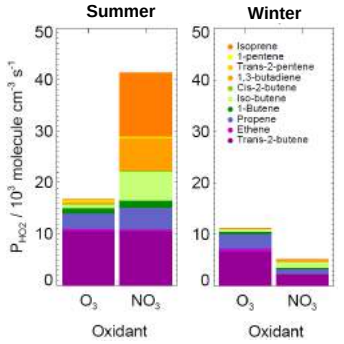

Figure 5: Rate of production of HO_2 (P_{HO2}) during summer (left) and winter (right) night-time flights, from reactions of NO_3 and O_3 with alkenes. Colour blocks represent contribution to HO_2 production from individual alkenes measured during the flights (given in legend, right).

5 Modelling

Overview of model results

- Mean model predicted OH concentration = 2.4×10^4 molecule cm^{-3} – this value is below the instrumental limit of detection in summer and winter (see table in section 4)
- Base model run **underpredicts HO_2*** and **overpredicts NO_3 and N_2O_5** (Figure 6)
- Radical production at night mainly due to reaction of NO_3 with VOCs
- Radical propagation is controlled by reaction of NO_3 with RO_2
- Radical loss occurs through HO_2 + RO_2 reactions, heterogeneous processes, and production of HNO_3 through OH + NO_2

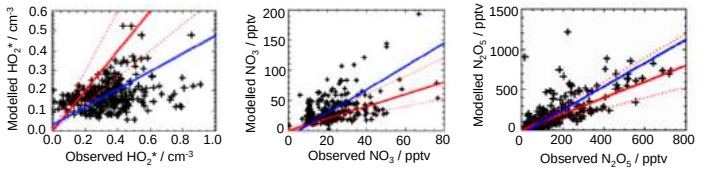

Figure 6: Comparison between modelled and observed concentrations of a) HO_2*, b) NO_3, c) N_2O_5 for the base MCM model run. Solid red line indicates the 1:1 line, with 50 % limits given by broken red lines. The best fit lines are shown in blue.

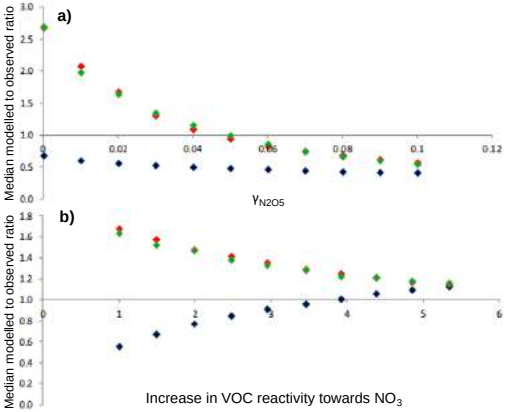

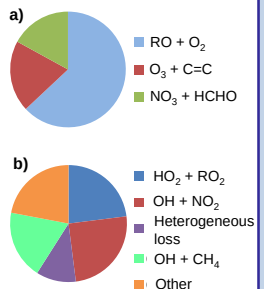

Figure 7: Processes controlling the instantaneous production (a) and loss (b) of HO_x (= OH + HO_2) radicals at night

Figure 8: Impact of γ_{N2O5} (a) and VOC reactivity (b) on the median modelled to observed ratios of HO_2* (blue), NO_3 (red) and N_2O_5 (green). a) Best fit values for NO_3 and N_2O_5 are achieved when γ_{N2O5} ~0.045; b) An increase of ~ 5 times the VOC reactivity towards NO_3 results in significant improvement to model prediction of HO_2, NO_3 and N_2O_5

6 Conclusions

- NO_3 + VOC chemistry is the most significant source of radicals in the model
- NO_3 + RO_2 dominates radical propagation
- Measurements and modelling both show strong coupling between NO_3 and HO_2 at night
- Improvements to model simulations for HO_2, NO_3 and N_2O_5 by inclusion of additional, unquantified unsaturated VOCs
- Inclusion of appropriate NO_3 + VOC and NO_3 + RO_2 chemistry is essential to successful model simulation of tropospheric night-time oxidation
- Increasing γ_{N2O5} to ~ 0.05 improves model prediction of NO_3 and N_2O_5, but further decreases modelled HO_2 concentrations

References

R. Commane, C. F. A. Floquet, *et al.*, *Atmos. Chem. Phys.*, 10, 8783-8801, **2010**
K. M. Emmerson and N. Carslaw, *Atmos. Environ.*, 43, 3220-3226, **2009**
K. M. Emmerson and M. J. Evans, *Atmos. Chem. Phys.*, 9, 1831-1845, **2009**
P. V. Forster, P. A. Ramaswamy *et al.*, Fourth Assessment Report of the IPCC, **2007**
H. Fuchs, B. Bohn *et al.*, *Atmos. Meas. Tech. Discuss.*, 4, 1255-1302, **2011**
A. Geyer, K. Bächmann *et al.*, *J. Geophys. Res. (Atmos.)*, 108, 8249-8264, **2003**
M. E. Jenkin, S. M. Saunders, *et al.*, *Atmos. Chem. Phys.*, 3, 181-193, **2003**
Y. Kanaya, Y. Sadanaga *et al.*, *Geophys. Res. Lett.*, 26, 2179, **1999**
T. Malkin, A. Goddard *et al.*, *Atmos. Chem. Phys.*, 10, 1441-1459, **2010**
X. Ren, H. Harder *et al.*, *Atmos. Environ.*, 37, 3639-3651, **2003**
X. Ren, W. Brune *et al.*, *Atmos. Environ.*, 40, 252-263, **2006**
S. Saunders, M. Jenkin , *et al.*, *Atmos. Chem. Phys.*, 3, 161-180, **2003**
R. Sommariva, M. J. Pilling *et al.*, *Atmos. Chem. Phys.*, 7, 587-598, **2007**
D. Stone, M. J. Evans *et al.*, *Atmos. Chem. Phys.*, 10, 9415-9429, **2010**

Acknowledgements NERC Grant No. NE/F004664/1

Thanks to NCAS, NERC and the RONOCO consortium including FAAM, B. Ouyang and O. Kennedy, University of Cambridge, for data in graphs presented in this poster.